International Journal of Rock Mechanics & Mining Sciences 146 (2021) 104887

Contents lists available at ScienceDirect

International Journal of Rock Mechanics and Mining Sciences

journal homepage: www.elsevier.com/locate/ijrmms

Development and application of cutterhead vibration monitoring system for TBM tunnelling

Fan Wu [a], Qiuming Gong [a,*], Zhigang Li [b], Haifeng Qiu [c], Cheng Jin [a], Liu Huang [a], Lijun Yin [a]

[a] Key Laboratory of Urban Security and Disaster Engineering of Ministry of Education, Beijing University of Technology, Beijing, 100124, China
[b] Sinohydro Bureau 1 Co., Ltd., Changchun, 130033, China
[c] Beijing Jiurui Technologies Co., Ltd., Beijing, 100107, China

ARTICLE INFO

Keywords:
TBM
Cutterhead vibration
Monitoring system
Penetration test
Engineering application

ABSTRACT

During TBM tunnelling, the rock breaking by cutters usually induces vibration. The cutterhead vibration is composed of all cutter vibrations. On the one hand, cutterhead vibration directly affects the life of the cutter, cutterhead and main gear. On the other hand, cutterhead vibration reflects the TBM excavation performance. In this paper, a cutterhead vibration monitoring system for TBM tunnelling was developed. The system consisted of the data acquisition module, communication and control module, as well as data processing and display module. Acceleration sensor, gyroscope and clock chip were integrated into a sensor board to acquire triaxial vibration data, cutterhead rotating status and acquisition time. The installation structure with anti-hit and water-proof functions was designed to ensure the stable operation of the system. Three types of data acquisition modes were proposed to meet the different monitoring scenarios. The system was applied in a TBM tunnelling project. Based on the normal monitored data in TBM tunnelling and penetration tests data, the differences in amplitude and frequency of triaxial vibration, as well as the effect of geological conditions and operating parameters on cutterhead vibration characteristics were analyzed. The engineering application showed that this system can reflect the changes of the geological conditions and operating parameters, providing guidance for the TBM tunnelling.

1. Introduction

TBMs have been extensively employed in urban rail transit due to their low project cost, high advance efficiency and safe work environment.[1] The cutterhead is located at the forefront of the TBM and it is one of the most important parts of the TBM. The violent vibration is generated during rock breaking by cutters. The cutterhead bears all the loads transmitted by the cutters, and its vibration is composed of all cutter vibrations. The cutterhead vibration was characterized as torsional and transverse vibrations of an elastomer under multi-point random impact loads.[2,3] Larger thrust, higher torque and stronger impact acted on the cutterhead system while TBM excavating in high-strength rock mass or mixed ground, inducing more severe vibration.[4] The cutterhead vibration usually induces some mechanical failures, such as bolt loosing, cutter abnormal wear, weld cracking and even cutterhead disintegration.[5–7] Cutterhead cracking caused by vibration was one of the key factors of cutterhead failures in some tunnel projects, such as Qinling Tunnel, DahuofangWater Diversion Tunnel and Zhongtianshan Tunnel.[8] The mechanical failures caused by vibrations led to lower construction efficiency, extended construction time and even serious safety accidents. Moreover, improper operation parameters, changes of geological conditions and unreasonable cutterhead layout also lead to abnormal vibration of the cutterhead.[9] Monitoring the cutterhead vibration is conducive to mastering the working status of the TBM and optimizing the operating parameters.

Based on theoretical analysis and numerical simulation, many scholars have conducted extensive studies on the vibration characteristics and influencing factors of the cutterhead. Li et al.[10] presented a dynamic two-dimensional nonlinear time-varying vibration model for the cutterhead driving system and found that the vibration amplitude was decreased by reducing the gear backlash, transmission error or torque. Ao and Zhang[11] suggested that the principal frequency of the cutterhead increased with the increase of the cutterhead diameter and stiffness based on the modal analysis theory of vibration structure. Ling et al.[12,13] established a coupling dynamic model of TBM split-cutterhead system based on Newmark-β's numerical integration method and

* Corresponding author.
E-mail address: gongqiuming@bjut.edu.cn (Q. Gong).

https://doi.org/10.1016/j.ijrmms.2021.104887
Received 15 April 2021; Received in revised form 7 June 2021; Accepted 25 August 2021
Available online 31 August 2021
1365-1609/

analyzed the influence of operating parameters, cutterhead piece mass and layout of main driving on the cutterhead vibration characteristics. The maximum relative error of the vibration amplitude between simulation and in-situ measured was close to 50%. Huo et al.[14] and Mei et al.[15] studied the influence of the support system on the vibration characteristics of TBM. The front support was effective in reducing the vibration amplitude and stabilization time of the cutterhead. The vibration acceleration on the main beam decreased as the structural size of the thrust cylinder increased. Sun et al.[3,16] found that the vibration amplitudes in the vertical direction of the cutterhead between cutterhead pieces and center block were almost the same. The cutterhead welds and flanged bolt joint were the easier damaged part under the violent vibration.

The structure of cutterhead is complex, and the coupling relationship of each component is difficult to establish. In addition, the cutterhead loads are difficult to accurately simulate due to the complex geological conditions. The vibration response obtained by numerical simulation or theoretical analysis is quite different from that of the cutterhead during TBM tunnelling. With the development of sensor and computer technology, assistant intelligence of TBM tunnelling has become a trend.[17] Cutterhead vibration monitoring becomes available and necessary. Liao[18] monitored the vibration signals of the TBM motor using an INV3080A equipment. The monitored data showed that the peak of the 4# pump station was 4.39 m/s and reached the alarm limit. Mooney et al.[19] and Walter[20] investigated the influence of operating parameters and geological conditions on vibration response by installing vibration sensors on the bulkhead. Impact-response testing indicated that vibration signals can be transferred from the cutterhead to the bulkhead. It should be noted that the vibration monitoring device was inapplicable to the cutterhead. Xin et al.[21] developed a vibration sensor VM-BOX for shield TBM, equipped with acceleration sensors with two ranges of 16 g and 200 g. The device was applied to Hefei Metro Line 3, but the vibration signal was disturbed by noise. Huang et al.[22] monitored the cutterhead vibration using a set of BeeTech A302EX acceleration sensors, and the monitored data was transmitted to the system software by wireless. The results showed that the most severe vibration was in the perpendicular direction to the cutterhead face, and the cutterhead vibration increased with the increase of cutterhead rotating speed and penetration rate. The similar results were found by Zhang et al.[23] However, the curves of the cutterhead vibration under different factors were not obtained. Huo et al.[24] and Ling et al.[25] installed the vibration sensor at the cutterhead manhole in the water diversion project of northwest Liaoning and proposed that the horizontal and vertical accelerations were affected by gravity during cutterhead rotating and the axial acceleration was not influenced.

In fact, a pressured chamber is located behind the cutterhead and the earth pressure reaches up to 2–3 bar. The muck is in direct contact with the monitoring device during EPB or slurry TBM tunnelling. The above-mentioned monitoring devices are not suitable for cutterhead due to the simple sensor protection structure, poor sealing, short battery life and unstable wireless communication. To realize the stable monitoring of cutterhead vibration, a cutterhead vibration monitoring system for TBM tunnelling was designed and developed. The developed system was applied to monitor the cutterhead vibration in a TBM tunnelling project. Based on the normal monitored data in TBM tunnelling, in-situ penetration tests data and the engineering geological conditions, the effect of operating parameters and geological conditions on vibration characteristics were studied.

2. System composition

The cutterhead vibration monitoring system consisted of three main modules, including the data acquisition module, communication and control module, as well as data processing and display module. The framework of the system was illustrated in Fig. 1. The data acquisition module included a triaxial acceleration sensor, gyroscope, clock chip, power supply and installation structure. The communication and control module was used to connect the system software and the data acquisition module. To realize the transmission of control commands and monitoring data, the module integrated an industrial switch, controller, and antenna. The main functions of the data processing and display module included the parse, storage, analysis and visualization of monitored data.

2.1. Data acquisition module

The pressured chamber of the EPB or slurry TBM is filled with muck in the soft soil ground during TBM tunnelling, resulting in unstable wireless signal transmission. During the tunnel construction, it takes a long time for segment installation and shutdown. Besides, the difference of geological conditions in each ring is small. That is to say, the cutterhead vibration monitoring for the entire tunnel construction is not necessary. Moreover, long-term continuous monitoring causes difficulty in data transmission and power consumption. The vibration response of the whole ring can be characterized by monitoring for several minutes in each ring. It not only obtains enough vibration information, but also

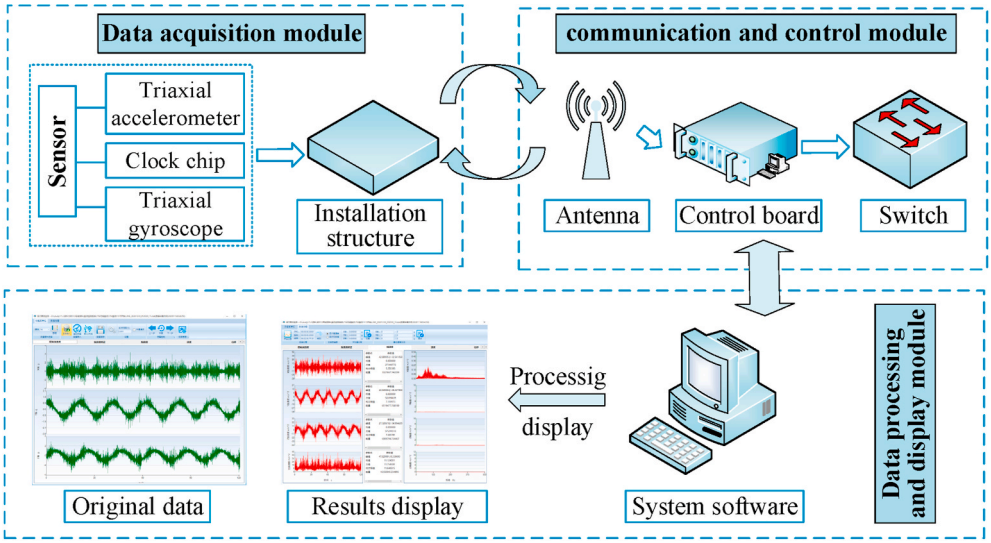

Fig. 1. System framework of the cutterhead vibration monitoring system.

prolongs the working time of the sensor. Based on the above consideration, three types of sensors were selected, including a triaxial vibration sensor, a triaxial gyroscope and a clock chip. The vibration sensor and gyroscope were integrated into a module with a size of 3 × 3 × 0.9 mm. The angle and rotation status of the cutterhead was obtained by the gyroscope. The acquisition time was determined by the clock chip.

The triaxial acceleration sensor was equipped with a proof mass for each axis. The acceleration was calculated by monitoring the displacement of the proof masses. Each axis worked independently. According to the actual working environment, the range of the acceleration sensor was adjusted to the maximum range of ±16 g. The specifications of the acceleration sensor and gyroscope were shown in Table 1.

To realize the long-time monitoring of cutterhead vibration, the low-power sensor board was designed. Besides sensors, the sensor board included button battery, memory card slot and various interfaces. The button battery supplied power to the clock chip. Different control programs were allowed to write to the sensor board through the writing interface for different monitoring needs. The communication between these sensors and the system software mainly depended on the communication interface. A rechargeable lithium battery with 16000mAh was designed to power the sensor board. The battery maintained continuous monitoring of the sensor board for 2–3 months.

On the basis of the working environment of the cutterhead, the installation structure was designed with the functions of anti-hit, anti-abrasion and water-proof, etc. as shown in Fig. 2. The installation structure was divided into the battery compartment, sensor board compartment and antenna compartment. To ensure the normal transmission of wireless signals, the Polytetrafluoroethylene (PTFE) material was used as the side panel of the antenna compartment. Waterproof connectors were adopted to connect each compartment. All the covers were set with seals for waterproof treatment. The thickened steel plates around the perimeter effectively protected the installation structure from damage. The installation structure was fixed on the cutterhead by welding.

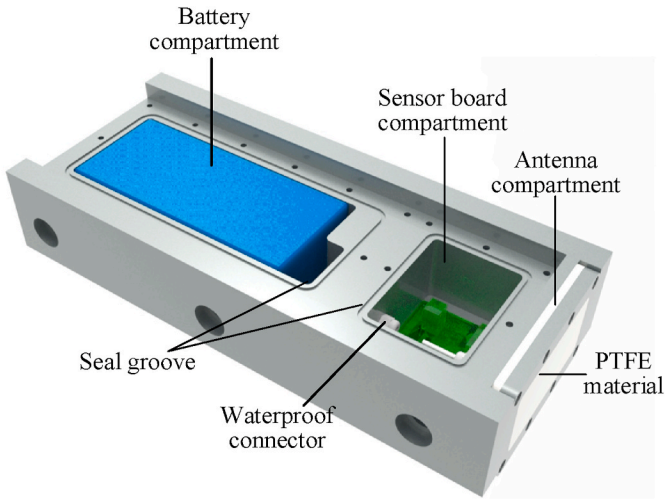

Fig. 2. Installation structure for data acquisition module.

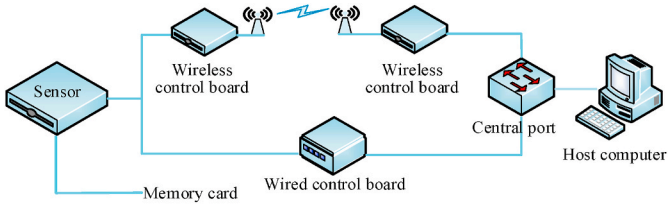

Fig. 3. Communication module.

2.2. Communication and control module

2.2.1. Communication module'

As a bridge between the data acquisition module and system software, the communication module was mainly responsible for the transmission of data and commands, as shown in Fig. 3. The wired and wireless transmission modes were designed. The wireless transmission mode adopted LoRa spread spectrum communication technology with the radio frequency (RF) of 433 MHz. It had the advantages of low power consumption, small size and ultra-long distance transmission. The wired transmission mode was mainly suitable for vibration monitoring of main drives, motors and other parts. The wired control board was connected to the sensor board and central port. The center part directly supplied power to the sensor board. To avoid data loss, all monitored data of the sensors can be stored in the memory card under two modes.

2.2.2. Control module

To synchronize the vibration monitoring with the TBM tunnelling, an automatic control program was designed. The automatic control program was of software control mode and sensor control mode for hard rock ground and soft soil ground, respectively. In the software control mode, the system software obtained the cutterhead rotation status from the programmable logic controller (PLC) of TBM. The software sent a data acquisition command to the sensor board after the cutterhead continued rotating for a few minutes. Then, the sensor board entered into the working status and was constantly monitored for a specific time. Then, the sensor board went into sleep mode to reduce power consumption. In the sensor control mode, the cutterhead rotation status was determined by the gyroscope. The angular velocity was greater than 0 during the cutterhead rotation. The subsequent control command was consistent with the software control mode. After the TBM was stopped, the monitored data was sent to the system software sequentially. In addition, the manual control mode was also embedded in the system software to meet the vibration monitoring under specific working conditions.

2.3. Data processing and visualization

2.3.1. Data processing

The main purpose of data processing is to obtain the time-domain and frequency-domain information of the vibration signal, as well as the vibration characteristic parameters. The data processing process was shown in Fig. 4. After receiving the monitoring data, the system software firstly parsed the data into triaxial acceleration and time, and then data were intercepted according to the analysis requirements. The sensor's errors, temperature changes and surrounding environmental disturbances cause noise and trend term in the monitored data. With the

Table 1
The specifications of sensors.

Sensor	Measuring range	Sensitivity scale factor	Noise	Sampling frequency	Operating voltage supply	Working temperature
acceleration sensor	±2, 4, 8, 16 g	16384, 8192, 4096, 2048 LSB/g	300 μg/√Hz	1000 Hz	1.71~3.5 V	-40~85 °C
gyroscope	±250, 500, 1000, 2000°/s	131, 65.5, 32.8, 16.4 LSB/(°/s)	0.01 dps/√Hz			

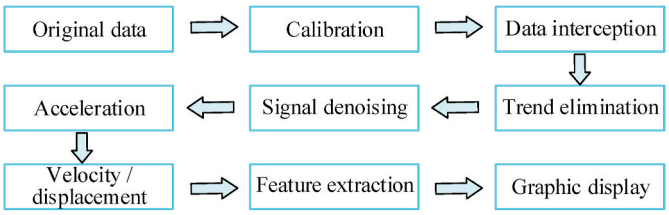

Fig. 4. Vibration data processing process.

existence of the trend term, the residual errors are amplified during the integration, resulting in waveform distortion. Currently, polynomial fitting is mostly used to eliminate the trend term. The system software was written in MATLAB, then the polyfit and polyval functions were called to implement polynomial fitting:

a = polyfit (t, x, m); % m-order polynomial fitting;
y = x-polyval (a, t); % polynomial numerical prediction;

where x is the original signal vector; y is the signal vector after eliminating the trend term; a is the polynomial coefficient; m is the order of the fitted polynomial and taken as 4; t is the discrete-time vector.

In general, the frequency of the noise signal is significantly different from the actual signal frequency, and the filter effectively reduces or eliminates the noise. By the above analysis, the expected results were obtained by combining polynomial fitting and filtering. Then, the velocity and displacement were obtained by primary and secondary integration of the acceleration.

Time-domain analysis and frequency-domain analysis of the vibration signal were embedded in the system software. The time-domain analysis represents the variation of acceleration with time and it is used to evaluate whether the vibration exceeds the bearing capacity or not. Frequency-domain analysis shows the frequency distribution of the structure. The frequency spectrum was obtained by fast Fourier transform of the vibration signal. Besides, some basic characteristic parameters of the vibration signal were also analyzed, such as extreme value, mean value, signal energy and so on, as shown in Table 2.

2.3.2. Software interface visualization

To manage a large amount of monitoring data, efficient visualization software was developed. The system software provided the following functions: data management, data processing, result display and user management. The software architecture was shown in Fig. 5. For example, the data management function mainly included data storage, historical data query and data input from the memory card. The result display function provided visualization of result data for acceleration, velocity, displacement, as well as the storage of result data and pictures. The system was developed by using Microsoft Visual Studio 2013 software and written in *C#* programming language. The data processing algorithm was based on MATLAB.

Fig. 6 showed the system software interface. The menu bar at the top of the main interface included data calibration, data input, automatic and manual acquisition, data storage, and user management, as shown

Table 2
Definition and description of vibration characteristics.

Parameters	Definition	Description
Extreme value, x_p	$\max(x')/\min(x')$	Maximum or minimum values of vibration signal
Mean value, $\overline{x'}$	$\sum x'/N$	Vibration signal average
Variance, σ^2	$\sum (x' - \overline{x'})^2/(N-1)$	Vibration signal dispersion degree
Signal energy, E	$\sum (x')^2$	Vibration signal energy level

Note: x' is the vibration signal vector after date processing; N is the number of x'.

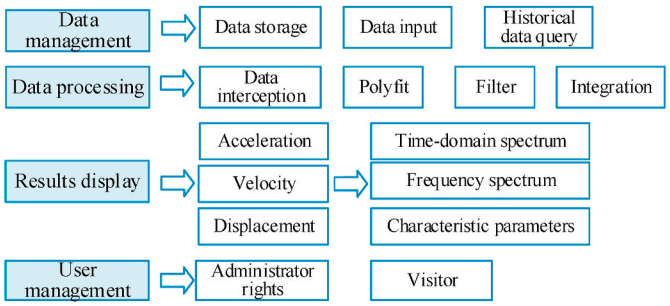

Fig. 5. Software architecture.

in Fig. 6 (a). The middle part contained buttons for original data, data processing, acceleration, velocity and displacement, which can be clicked to enter different sub-interfaces. The original vibration monitoring data was shown at the bottom of the interface. The acceleration sub-interface was shown in Fig. 6 (b), displaying the acceleration processing results. The time-domain spectrum, characteristic parameters and frequency spectrum were displayed on the left, middle and right, respectively. The layout of the velocity and displacement sub-interfaces was similar to that of the acceleration sub-interface.

3. System verification

To verify the reliability and accuracy of the cutterhead vibration monitoring system, the system was set up and tested indoors, as shown in Fig. 7. A rotating platform was developed to simulate the TBM cutterhead. The sensor board was fixed on the rotating platform. The rotating platform drove the sensor board to rotate while turning on the motor. The rotating speed was adjustable.

Before the system tests, the control program and time information were written into the sensor board. The sensor board was adjusted to the horizontal position, in other words, Z+ is vertical down. The rotating platform was stationary and the sensor signal was collected continuously for 100 s by manual control. The vibration monitoring data for the static state was shown in Fig. 8 (a). The Z-axis acceleration was close to the gravitational acceleration, and the X-axis and Y-axis fluctuated around an initial value. The error in the initial value can be eliminated by the system software. The fluctuation amplitude was small, basically within 0.05 m s^{-2}, and there was no abnormal value. Similar results were obtained by changing the orientation of the sensor board. This test was also conducted by Huang et al.[22] to verify the reliability of the vibration sensor.

Turning on the rotating platform and adjusting the rotating speed to 5 rpm, the verification test was performed according to the sensor control mode of the monitoring system. Fig. 8 (b) showed the monitored data in the rotating state. The X-axis acceleration fluctuated around 0, and the Y-axis and Z-axis showed periodic variations with a period of 12 s. The combined accelerations of the Y-axis and Z-axis at any moment were approximately equal to the gravitational acceleration with the platform rotation. The fluctuations of the vibration acceleration were mainly affected by the rotating platform. The results showed that the vibration monitoring system worked normally and the monitored data was reliable.

4. Engineering application

4.1. Project overview

The cutterhead vibration monitoring system was installed to a dual-mode shield TBM at Shenzhen Metro Line 12 from Huaide station to Fuyong station. The total length of the right line is about 1750 m, and the tunnel depth is 10~110 m. The segment used in the tunnel has an outer diameter of 6.2 m, an inner diameter of 5.5 m and a width of 1500

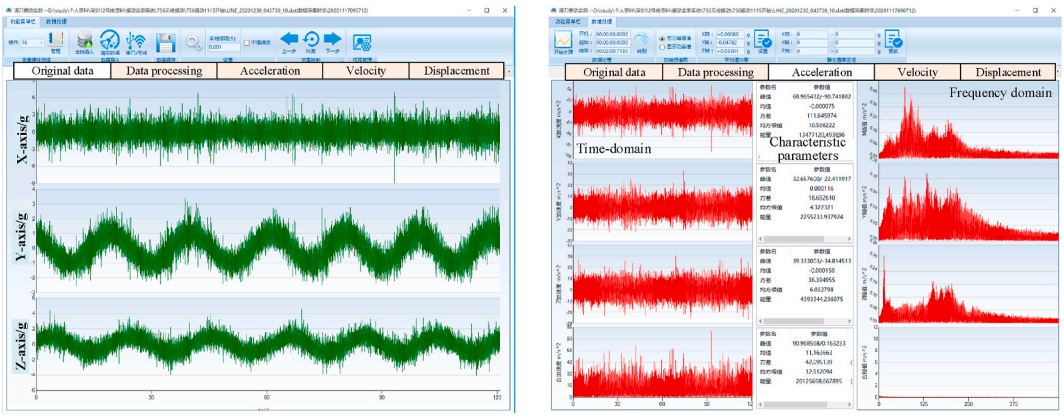

(a) Main interface (b) Acceleration sub-interface

Fig. 6. System software interface.

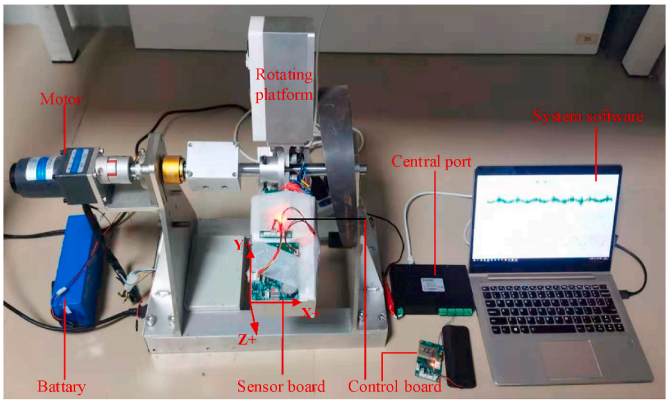

Fig. 7. System assembly and validation.

mm. Fig. 9 presented the geological profile along the tunnel alignment. The excavated grounds in the tunnel section included soft soil, hard rock, mixed ground and fault zone. The hard rock is mainly composed of slightly weathered migmatitic granite with a length of more than 1000 m. A dual-mode shield TBM was manufactured by China Railway Engineering Equipment Group Co. Ltd. to achieve high advance rate under different grounds, as shown in Fig. 10. The dual-mode shield TBM had EPB mode and TBM mode.[26] The EPB mode was applicable to soft soil with the screw conveyor, and the TBM mode was suitable for hard rock with the conveyor belt. The cutterhead had a diameter of 6.47 m and was equipped with 47 disc cutters and 68 scrapers, including 6 central cutters, 23 face cutters and 12 gauge cutters. The design specifications of the shield TBM were shown in Table 3.

4.2. *System installation and engineering verification*

4.2.1. *System installation*

The location of the sensor installation should not disturb the cutter replacement and cutterhead mucking. The installation structure was welded on the spoke behind the scraper with a radius of 2.5 m, as shown in Fig. 11. It should be noted that the X-axis was perpendicular to the tunnel face, the Y-axis and Z-axis were parallel to the tunnel face. The Y-axis was the radial direction and the Z-axis was the tangential direction. To enhance signal transmission, the antenna compartment was oriented towards the door of the pressured chamber. The central port and the control board were fixed on the back of the pressurized chamber. The antenna connected to the control board was inserted into the pressurized chamber through a pre-hole. The system software was installed on the host computer in the operation room and was connected to the central

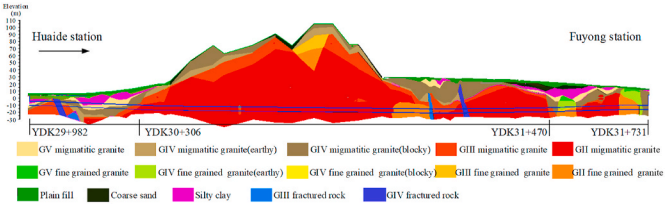

Fig. 9. Geological profile along the tunnel alignment.

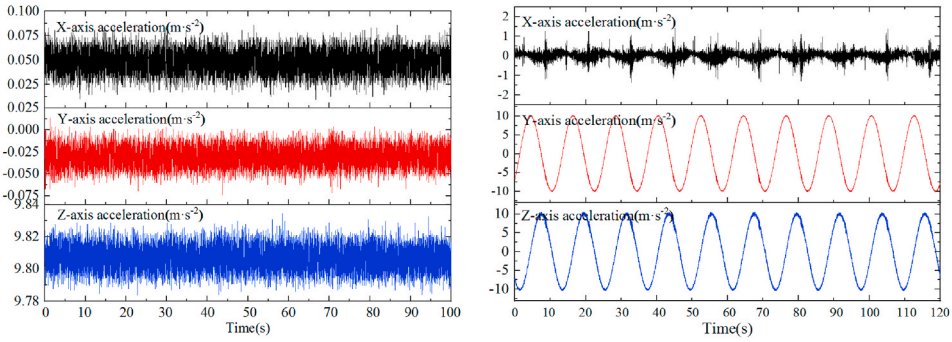

(a) Monitoring data for static state (b) Monitoring data for rotating state

Fig. 8. System verification results for static and rotating states.

Fig. 10. Dual-mode shield TBM used in the section from Huaide station to Fuyong station.

Table 3
Specifications of dual-mode shield TBM.

Technical parameters	Design value
Cutterhead diameter	6470 mm
Opening rate	28%
Cutterhead power	1750 kW
Rated torque	6686 kN m
Cutterhead rotating speed	0-2.5-5 r/min
Maximum thrust	4086T
Maximum advance speed	80 mm/min
Type of cutter	18in-457mm
Number of cutters	49
Cutter spacing	75 mm
Number of scrapers	68

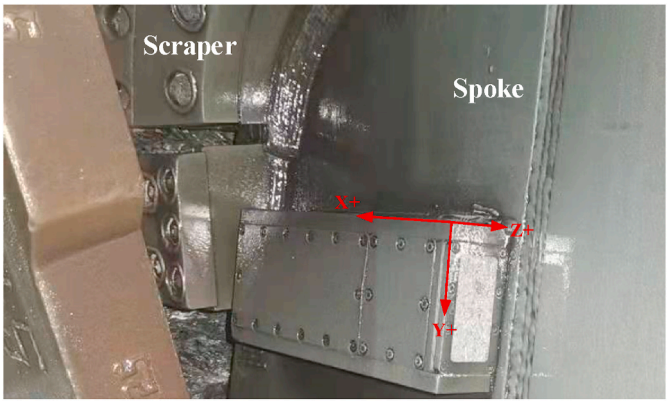

Fig. 11. Installation structure on the cutterhead spoke behind the scraper.

port through a network cable. The layout of the monitoring system on site was shown in Fig. 12.

The dual-mode shield TBM started in EPB mode on March 30, 2020. After the shield TBM entered the hard rock, the mode change was carried out on June 20. In TBM mode, the sensor was installed on November 1, 2020, and then the system worked normally.

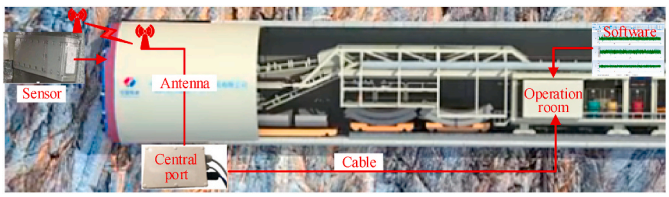

Fig. 12. System layout in the shield TBM.

4.2.2. Engineering verification

The further validation of the field monitored data of the system was conducted due to the complex working environment of the cutterhead.

Fig. 13 showed the triaxial acceleration under cutterhead rotation without tunnelling after the system was installed, and the cutterhead rotating speed was about 3 rpm. The cutterhead hit the rock fragments, tunnel wall and tunnel face causing local fluctuations. The local fluctuation amplitudes were relatively small, which can be more intuitive to analyze the triaxial vibration trend. The X-axis was not affected by the cutterhead rotated and the acceleration fluctuated around the value of 0. The Y-axis and Z-axis accelerations showed periodic variation with a period of 20s and were consistent with the cutterhead rotating speed. The sensor rotated continuously as the cutterhead rotated, as shown in Fig. 14. The gravity components of the Y-axis and Z-axis changed with the sensor angle variation, which showed a phase difference of 90°. In addition, the Y-axis was also subjected to centripetal acceleration caused by cutterhead rotation, but the value was very small (0.25 m s^{-2} in the field test). That was to say, the overall fluctuations of the Y-axis were expressed as centripetal acceleration and gravity components, that of the Z-axis were expressed as gravity components, as shown by the red line in Fig. 13, and the local fluctuations were caused by rock breaking and hitting. The triaxial vibration trend of the cutterhead was basically consistent with the results by Ling et al.[25] and Huo et al.[24] during TBM tunnelling.

Based on the above analysis, it was clear that the triaxial vibration trend was reasonable and conformed to the actual engineering. In conclusion, the monitoring system in this paper was reliable and accurate.

4.3. Differences in triaxial vibration

Fig. 15 showed the typical triaxial vibration acceleration of the cutterhead during TBM tunnelling. The monitored data was obtained at the Chainage K31 + 107 on November 17, 2020, and the rock mass on the tunnel face was slightly weathered migmatitic granite.

After the gravity components of the Y-axis and Z-axis were

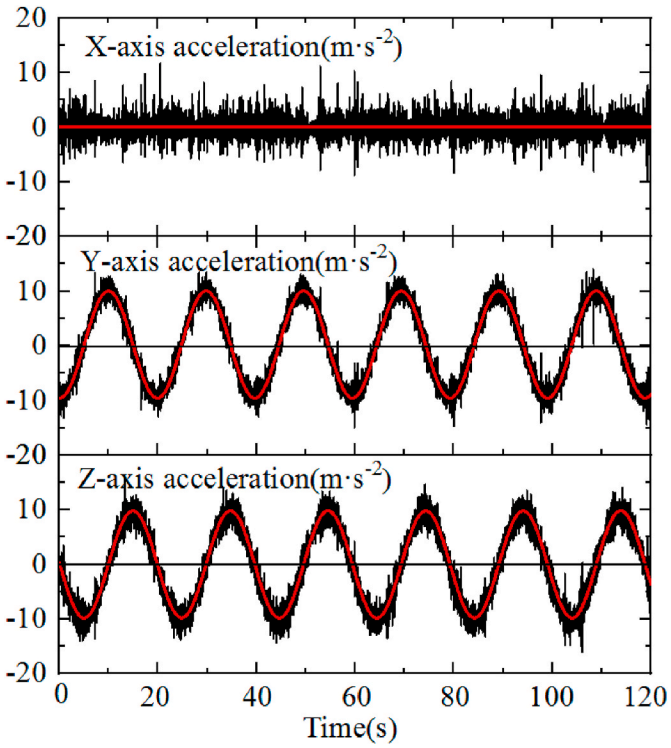

Fig. 13. Triaxial acceleration under cutterhead rotation without tunnelling.

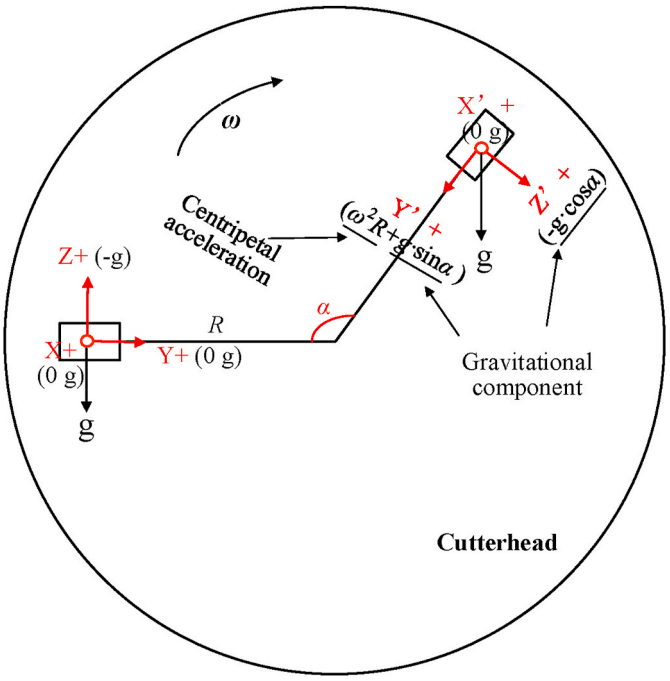

Fig. 14. The gravity components with the sensor angle variation. (ω is the angular velocity, m·s^{-1}; R is the sensor installation radius, m; g is gravitational acceleration, m·s^{-2}).

eliminated by the high-pass filter, the extreme values of triaxial acceleration were 77.4/-79.6, 30.9/-27.6 and 38.0/-40.4 m s^{-2}, respectively, and the mean values were close to 0. The signal energy of the cutterhead vibration for triaxial were 1.42, 0.76 and 1.01 × 10^{7}, respectively. The vibration intensity in the X-axis was the most violent and the amplitude was close to 2 times of the other two directions. Similar results were found by Huang et al.[22] and Zhang et al.[23] Combined with the rock breaking mechanism by the cutter, the stress concentration occurred in the contact area between the cutter and rock during the rock breaking. The radial cracks gradually propagated and coalesced between the adjacent cutters. Then the rock fragment was generated and popped out, resulting in a groove under the cutter. The stress of the cutter quickly released and the vibration was formed. The cutter force in the X-axis was the largest, the vibration was the most violent. That is to say, the effect of thrust or penetration rate on cutterhead vibration was greater than that of the torque. In addition, the violent vibrations in the X-axis were more likely to damage the cutterhead system. Therefore, the subsequent analysis focused on the X-axis of the cutterhead.

The frequency-domain analyses were shown in Fig. 15 (b). The vibration frequency of the X-axis was concentrated in the range of 50~200 Hz. The principal frequency was about 90 Hz with an amplitude of 0.5 m s^{-2}, and the other frequencies were distributed around 75 Hz and 115 Hz. The principal frequency and amplitude of the Y-axis and Z-axis were consistent with the cutterhead rotating frequency and gravitational acceleration, respectively. The frequency was around 0.05 Hz and the amplitude was close to 9.8 m s^{-2}. The principal frequency of the X-axis generally did not change with the operating parameters, but the principal frequency of the Y-axis and Z-axis was equal to the cutterhead rotating frequency.

4.4. *Influence of the geological conditions on cutterhead vibration*

Between November 16, 2020 and November 19, 2020, the TBM tunneled through a fault zone, namely from slightly weathered fine-grained granite to fault zone, and then to slightly weathered migmatitic granite. The uniaxial compressive strengths of the fine-grained granite and migmatitic granite are 110.5 and 97.5 MPa, respectively. The fault zone is composed of highly to moderately weathered fractured rock mass.

Fig. 16 showed the X-axis acceleration at different rock masses. The X-axis acceleration was defined as the average of the absolute values of 10 extreme points for each set of the monitored data. The rock mass boreability index was calculated by dividing thrust per cutter by penetration rate. The higher the boreability index is, the rock breaking is more difficult. During TBM tunneling at the fault zone, the X-axis acceleration decreased rapidly from 60 m s^{-2} to 30 m s^{-2}, and then gradually increased to 50 m s^{-2}. Moreover, the X-axis in the fine-grained granite was more severe than that of the migmatitic granite. That is to say, the geological conditions had an obvious influence on the cutterhead vibration intensity. The vibration amplitude increased with the increase of rock compressive strength. In the hard rock ground, it was difficult to break the rock mass by cutters. The cutter force increased with the increase of the rock compressive strength, resulting in more intense vibrations during rock breaking. The rock mass in the fault zone was loose and poor in integrity. The cutters broke the rock mass easily with a smaller boreability index, so the vibration was weaker.

Based on the above analysis, the cutterhead vibration acceleration

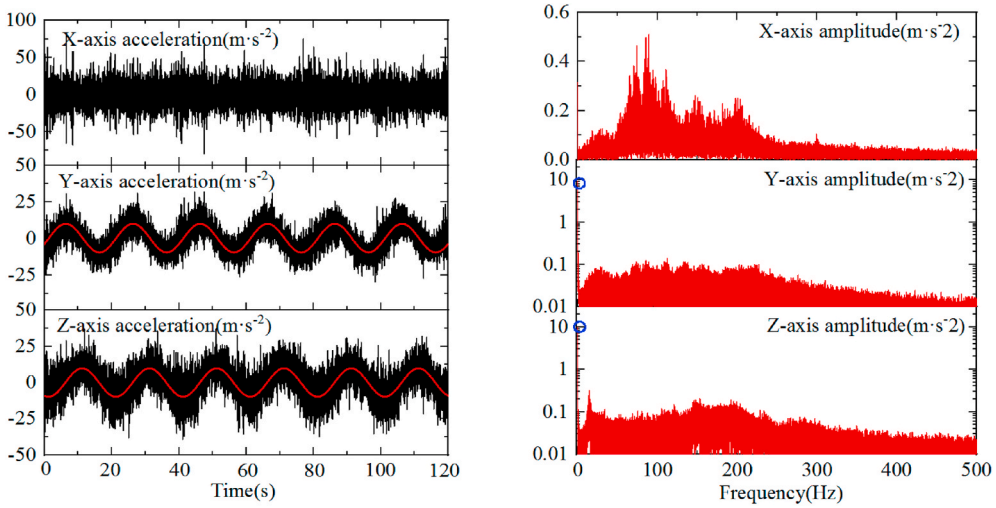

(a) Time-domain analyses (b) Frequency-domain analyses

Fig. 15. Typical triaxial vibration of cutterhead during TBM normal tunnelling

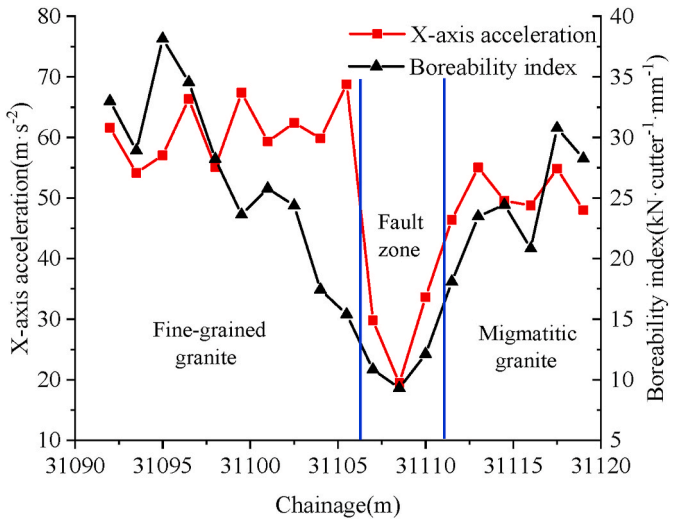

Fig. 16. X-axis acceleration and rock mass boreability index in different geological conditions.

can be used as a preliminary parameter to determine the geological condition of the tunnel face. For example, the TBM may go through a fault zone or highly weathered rock mass when the X-axis acceleration is less than 30 m s^{-2}.

4.5. Influence of operating parameters on cutterhead vibration

4.5.1. In-situ TBM penetration tests

The change of the operating parameters can directly affect the vibration response of the cutterhead. A series of in-situ TBM penetration tests were conducted to investigate the influence of cutterhead thrust and rotating speed on cutterhead vibration. The penetration tests were performed at the Chainage K31 + 010 m on November 5, 2020. The rock mass in the test site was migmatitic granite and belonged to intact rock mass, as shown in Fig. 17. Before the tests, all cutters were checked out and in normal wear condition.

For the tests of different cutterhead thrusts, the cutterhead rotating speed was maintained at 3 rpm. The six test steps were designed according to the thrust levels. Each step lasted around 10min and 30 kg of rock debris was collected. For the tests of different cutterhead rotating speeds, six test steps were carried out and the cutterhead thrust was controlled at about 13000 kN. The cutterhead vibration was continuously monitored by manual control mode during the tests. The operating parameters of the whole test process were shown in Fig. 18. The results of the tests were listed in Table 4.

Fig. 17. Photos of the tunnel face at the test site.

4.5.2. Relationship between cutterhead thrust and vibration amplitude

There was a critical value of cutterhead thrust that divided the growth of the X-axis acceleration into two stages, as shown in Fig. 19. For the cutterhead thrust below the critical value, the X-axis was essentially constant with the increase of cutterhead thrust. Then, the X-axis acceleration increased rapidly with the increase of the cutterhead thrust. Besides, the X-axis acceleration increased almost linearly with the increase of the penetration rate, as shown in Fig. 20.

In general, the stress acting on the cutter increases with the increase of the penetration rate. At the same time, the cutterhead vibration is more serious. The interaction of the adjacent cutters was weaker under a lower cutterhead thrust, the penetration rate did not change significantly and the vibration was moderate as the cutterhead thrust increased. In contrast, after the cutterhead thrust exceeded the critical value, the larger thrust accelerated the crack propagation under the cutters. Therefore, the vibration amplitude increased rapidly as the penetration rate increased.

4.5.3. Relationship between excavation efficiency and vibration signal energy

The coarseness index is related to the excavation efficiency. The larger roughness index indicates more rock fragments and higher excavation efficiency. There was a good linear correlation between coarseness index, vibration signal energy and penetration rate, as shown in Fig. 21. With the increase of the penetration rate, more rock fragments were produced during rock breaking, resulting in higher TBM excavation efficiency. Moreover, the formation of rock fragments was generally accompanied by the cutterhead vibration. The cutterhead vibration became more frequent and more violent with the increase of the rock fragments, so the vibration signal energy was increased. Therefore, the vibration energy may also be used to characterize the excavation efficiency.

4.5.4. Effect of cutterhead rotating speed on vibration amplitude

Fig. 22 showed the variation of the cutterhead X-axis acceleration at different cutterhead rotating speeds. There was a critical value of the cutterhead rotating speed with a value of 3.5 rpm. As the cutterhead rotating speed was less than the critical value, the vibration amplitude of the cutterhead increased rapidly with the increase of the cutterhead

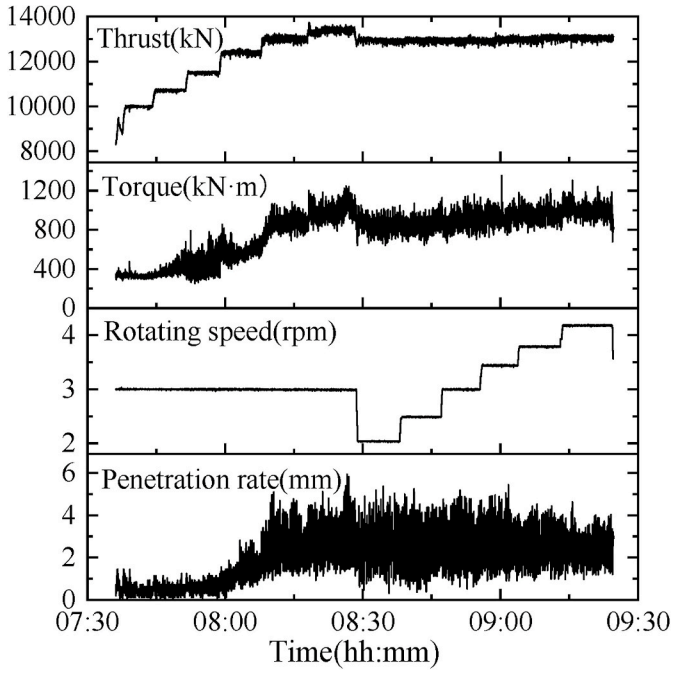

Fig. 18. Variation of operating parameters with time under penetration tests.

Table 4
Penetration tests results.

Different thrust tests	Test step	1–1	1–2	1–3	1–4	1–5	1–6
	Thrust (kN)	9991	10729	11498	12402	13019	13391
	Torque (kN·m)	328.1	384.2	442	570.3	853.8	991.8
	Rotating speed (rpm)	3	3	3	3	3	3
	Penetration rate (mm)	0.43	0.48	0.59	1.25	2.41	2.83
	Test time (min)	6	7	7	8.5	11.5	10
	Coarseness index	411.5	434.6	419.6	487.9	563.4	580.4
	X-axis acceleration ($m{\cdot}s^{-2}$)[a]	33.2	33.6	34.0	40.8	50.4	60.4
	X-axis signal energy (10^7)[b]	0.14	0.15	0.14	0.80	2.34	3.08
Different rotating speed tests	Test step	2–1	2–2	2–3	2–4	2–5	2–6
	Rotating speed (rpm)	2	2.5	3	3.4	3.8	4.2
	Thrust (kN)	12939	12943	12934	12967	13022	13043
	Torque (kN·m)	842.8	851	881	921.8	953.2	1000
	Penetration rate (mm)	2.5	2.5	2.6	2.6	2.5	2.4
	Test time (min)	9	8.5	8	7.5	9	10.5
	X-axis acceleration ($m{\cdot}s^{-2}$)	44.9	50.4	55.8	65.7	66.1	65.0

Note.
[a] X-axis acceleration was defined as the average of the absolute values of 20 extreme points for the monitoring data of each step.
[b] X-axis signal energy is the accumulation of signal energy for 6 consecutive minutes.

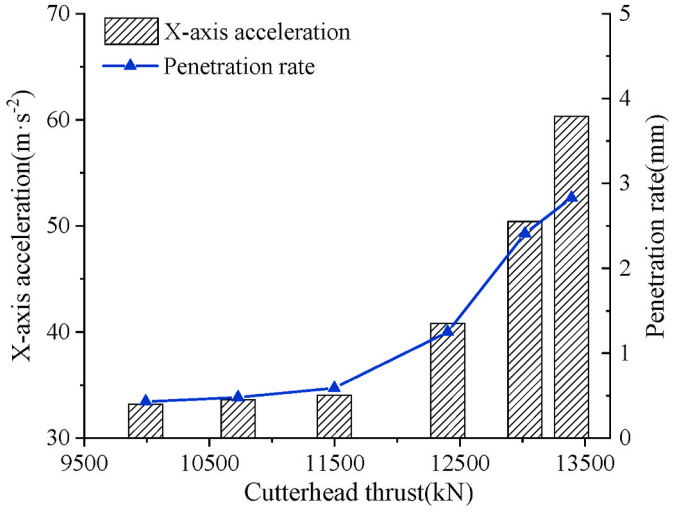

Fig. 19. Effect of penetration rate and cutterhead thrust on X-axis acceleration.

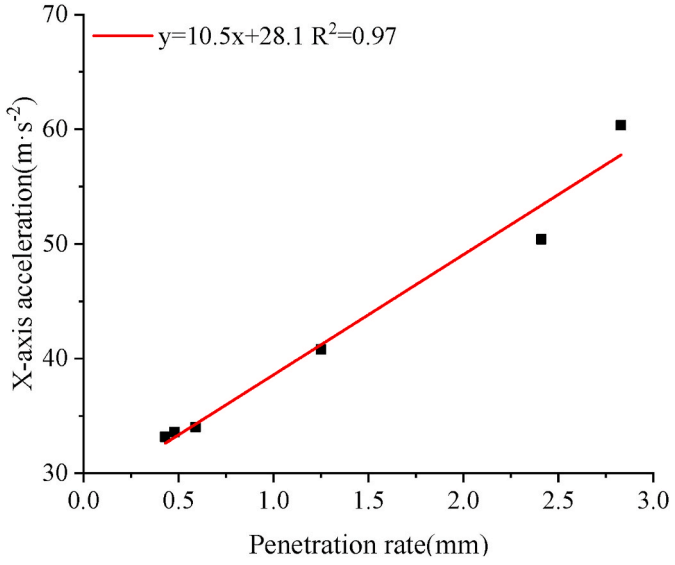

Fig. 20. Relationship between X-axis acceleration and penetration rate.

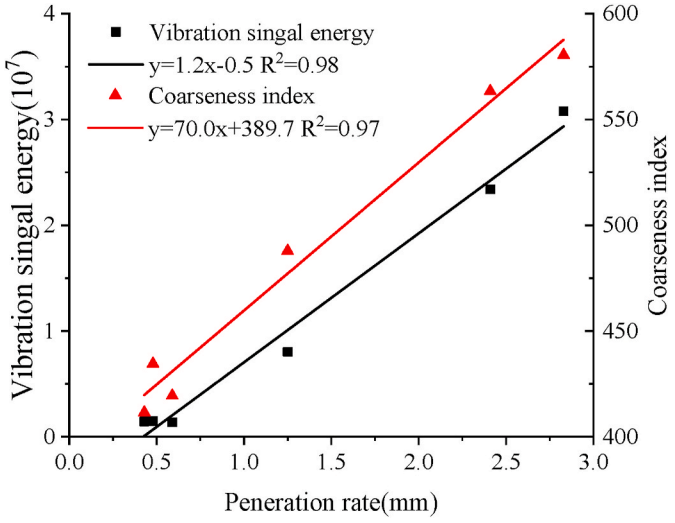

Fig. 21. Relationship between vibration signal energy, coarseness index and penetration rate.

rotating speed. In general, the rock fragments were formed by several times of rock breaking by the cutters. The cutter broke the rock more times in the same time under higher cutterhead rotating speed. More rock fragments presented more intense and more frequent vibrations. However, the vibration amplitude was almost constant until the cutterhead rotating speed exceeded 3.5 rpm.

Based on the above analysis, the TBM operating parameters and geological conditions have significant influence on cutterhead vibration, and the curves of the cutterhead vibration under different factors were presented. The monitored data of cutterhead vibration may be used to optimize the TBM operating parameters and prevent severe vibration from affecting the cutter, cutterhead and main gear life. In addition, the changes in the geological conditions may be determined based on the vibration amplitude, so early warning of adverse geological hazards is necessary. It should be noted that the TBM specification parameters are quite different in various tunnel projects, such as cutterhead stiffness and cutter layout. The specific values in this paper are only applicable to this tunnel section. That is to say, cutterhead vibration monitoring in different tunnel projects is essential. Moreover, despite the developed system showed satisfactory performance in the engineering application, unstable wireless data transmission often caused data loss in the data transmission. In the following research, data transmission efficiency will

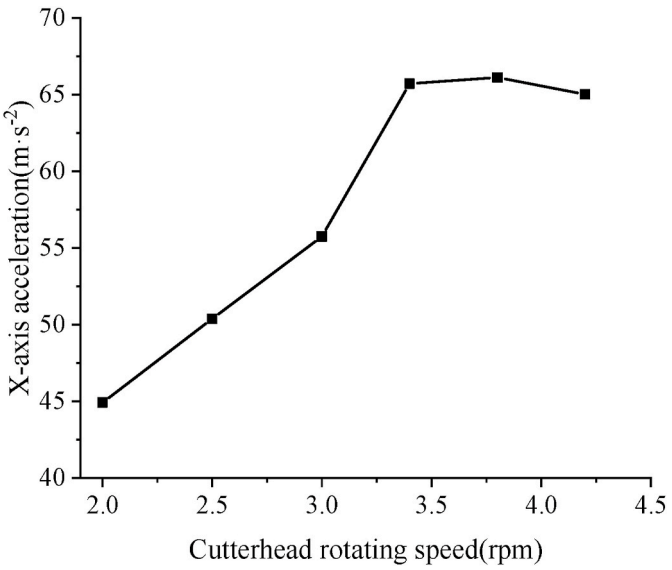

Fig. 22. Effect of cutterhead rotating speed on X-axis acceleration.

be the focus of system improvement. Besides, the mechanism and engineering logic of cutterhead vibration are worth studying and will be carried out in the future. The monitoring system will be installed on the linear cutting machine to detected the cutter vibration characteristic during cutting tests. Combined with test data and theoretical analysis, the mechanism of cutter vibration, as well as the relationship between cutter vibration and cutterhead vibration will be studied. In addition, the evaluation of TBM operation status based on the vibration data is also a key problem.

5. Conclusions

A cutterhead vibration monitoring system for TBM tunnelling was developed in this paper. The system consisted of the data acquisition module, communication and control module, as well as data processing and display module. The acceleration sensor, gyroscope, and clock chip were integrated into the data acquisition module. The installation structure was designed to meet the long-term vibration monitoring of system. A rotating platform was developed to verify the workability of the system. The static and rotating tests were performed in the rotating platform. The test results showed that the monitored data of the system is reliable.

The developed monitoring system was applied to a tunnel project. Besides, the normal monitoring data in TBM tunneling, a series of in-situ TBM penetration tests were conducted to study the cutterhead vibration response. By analyzing the monitored data, the vibration intensity in the X-axis was larger than the other two directions. The vibration amplitude decreased significantly while TBM went through a fault zone. The penetration rate increased rapidly and the cutterhead vibration became more serious after the cutterhead thrust exceeded the critical value. The X-axis acceleration increased nearly linear with the penetration rate. In terms of the cutterhead rotating speed, the vibration amplitude increased substantially with increasing cutterhead rotating speed, and then remained unchanged after the cutterhead rotating speed exceeded 3.5 rpm.

Declaration of competing interest

The authors declare that they have no known competing financial interests or personal relationships that could have appeared to influence the work reported in this paper.

Acknowledgments

We are grateful to Sinohydro Bureau 1 Co., Ltd for the cooperation in the in-situ application of the system.

References

1 Gong QM, Wu F, Wang DL, Qiu HF, Yin LJ. Development and application of cutterhead working status monitoring system for shield TBM tunnelling. *Rock Mech Rock Eng.* 2021;54:1731–1753.
2 Schlangen E, Mier JGMV. Simple lattice model for numerical simulation of fracture of concrete materials and structures. *Mater Struct.* 1992;25(9):534–542.
3 Sun W, Zhu Y, Wang WZ, Zhu D. Evaluation of TBM cutterhead vibration under complicated condition. In: *2016 12th IEEE/ASME International Conference on Mechatronic and Embedded Systems and Applications (MESA)*. IEEE; 2016.
4 Huo JZ, Sun XL, Li GQ, Li T, Sun W. Multi-degree-of-freedom coupling dynamic characteristic of TBM disc cutter under shock excitation. *J Cent South Univ.* 2015;22(9):3326–3337.
5 Bayati M, Hamidi JK. A case study on TBM tunnelling in fault zones and lessons learned from ground improvement. *Tunn Undergr Space Technol.* 2017;63:162–170.
6 Bilgin N. An appraisal of TBM performances in Turkey in difficult ground conditions and some recommendations. *Tunn Undergr Space Technol.* 2016;57(Aug):265–276.
7 Qi MX, Li HL, Wang YJ. Research and application of refit technology of all-section rock tunnel boring machine. *Constr Mach Technol Manag.* 2009:97–102, 03.
8 Li JB, Zhang ZG, Meng ZC, Huo JZ, Xu ZH, Chen J. Tunnel boring machine cutterhead crack propagation life prediction with time integration method. *Adv Mech Eng.* 2019;11(6), 168781401985345.
9 Rostami J. Hard rock TBM cutterhead modeling for design and performance prediction. *Geomech Tunn.* 2008;1(1):18–28.
10 Li XH, Yu HB, Zeng P, Yuan MZ, Sun LX, Zhao Y. Dynamic two-dimensional nonlinear vibration modeling and analysis for shield TBM cutterhead driving system. *Trans Can Soc Mech Eng.* 2014;38(4):417–463.
11 Ao RH, Zhang YT. Analysis of cutter disc vibration in shield driving. *J Mach Des.* 2010;27(2) (in Chinese).
12 Ling JX. *Vibration Analysis and Life Prediction of TBM Cutterhead under Spatially-Distributed Loads*. Liaoning: Dalian University of Technology; 2015, 2015.
13 Ling JX, Sun W, Huo JZ, Deng LY. Sensitivity of vibration response about TBM cutterhead system with multi-degree-of-freedom coupling. *J Cent South Univ.* 2017;48(3):650–657.
14 Huo JZ, Ouyang XY, Zhang X, Jing C. The influence of front support on vibration behaviors of TBM cutterhead under impact heavy loads. *Appl Mech Mater.* 2014;541–542:641–644.
15 Mei YB, Xia YM, Lin LK, Cheng YL, Qian C. Influence factors of vibration response on supporting-thrusting system of tunnel boring machine. *Math Probl Eng.* 2020;(7):1–10.
16 Sun Wei, Ling JX, Huo JZ, Guo L, Zhang X, Deng LL. Dynamic characteristics study with multidegree-of-freedom coupling in TBM cutterhead system based on complex factors. *Math Probl Eng.* 2013:1–17.
17 Zhou XX, Gong QM, Liu YQ, Yin LJ. Automatic segmentation of TBM muck images via a deep-learning approach to estimate the size and shape of rock chips. *Autom ConStruct.* 2021;126(5), 103685.
18 Liao JW. Test and analysis on vibration detection of TBM equipment in urban rail transit engineering. *Railway Const Technol.* 2016;(6):84–86 (in Chinese).
19 Mooney M, Walter B, Steele J, Cano D. Influence of geological conditions on measured TBM vibration frequency. In: *Proceedings of 2014 North American Tunneling Conference*. 2014.
20 Walter BW. *Detecting changing geologic conditions with tunnel boring machines by using passive vibration measurements*. PhD Thesis. USA: Colorado School of Mines; 2013.
21 Xin SJ, Zhou YH, Zhang M, Li lei. Research and development of shield-/TBM-dedicated vibration monitoring sensor VM-BOX, 04 *Tunn Constr.* 2018;213:197–202 (in Chinese).
22 Huang X, Liu QS, Liu H, et al. Development and in-situ application of a real-time monitoring system for the interaction between TBM and surrounding rock. *Tunn Undergr Space Technol.* 2018;81:187–208.
23 Zhang XP, Liu QS, Zhang JM. Real-time monitoring technology for wear of cutters and monitoring and analysis of cutterhead vibration of TBM. *Tunn Constr.* 2017:135–140, 03.
24 Huo JZ, Wu HY, Yang J, Sun W. Multi-directional coupling dynamic characteristics analysis of TBM cutterhead system based on tunnelling field test. *J Mech Sci Technol.* 2015;29(8):3043–3058.
25 Ling JX, Sun W, Yang XJ, Tong X, Zhang N. Vibration response and parameter influence of TBM cutterhead system under extreme conditions. *J Mech Sci Technol.* 2018;32(10):4959–4969.
26 Burger W. Multi-mode tunnel boring machines/Multi-Mode Tunnelvortriebsmaschinen. *Geomech Tunn.* 2014;7(1):18–30.